Supporting Information

Reductive Amination of Ethyl Levulinate to Pyrrolidones over AuPd Nanoparticles at Ambient Hydrogen Pressure

Michelle Muzzio, Chao Yu, Honghong Lin, Typher Yom, Dilek A. Boga, Zheng Xi, Na Li, Zhouyang Yin, Junrui Li, Joshua A. Dunn, Shouheng Sun*

Materials

Palladium acetylacetonate ($Pd(acac)_2$) and gold tetrachloroaurate ($HAuCl_4$) were purchased from Strem Chemicals. Oleylamine (technical grade, 70%), ethyl levulinate (99%), levulinic acid (98%), oleic acid (technical grade, 90%), ammonia borane (90%), mesitylene (98%), 1,2,3,4-tetrahydronaphthalene (tetralin, 99%), copper acetylacetonate ($Cu(acac)_2$), and borane tert-butylamine (97%), octylamine (99%) and other amines used in this work were all from Sigma Aldrich. Borane morpholine (97%) was from Alfa Aesar. Hydrogen was purchased from Corps Brothers and was UHP 99.999%. Hexane (98.5%), isopropanol (100%), ethanol (100%), methanol (100%) and acetic acid (98%) were purchased from Fisher Scientific. All reagents were used as received.

Nanoparticle (NP) Synthesis

The NP syntheses were carried out using standard airless procedures and commercially available reagents.

Synthesis of AuPd Alloy NPs. AuPd alloy NPs were synthesized through adaption of a previously published synthesis.[1] $Au_{66}Pd_{34}$ NPs were synthesized by first dissolving 0.08 g of $HAuCl_4$ and 0.032 g $Pd(acac)_2$ in 4 mL of oleylamine (OAm) through shaking and gentle vortexing. 200 mg borane morpholine was dissolved in 10 mL OAm and degassed in a reaction flask with nitrogen or argon at 70 ˚C for a half hour. The solution of $HAuCl_4$, $Pd(acac)_2$, and oleylamine was rapidly injected into the reaction flask (turned black within seconds). The temperature was raised to 220 ˚C at a rate of 3-5 ˚C/min. After 30 min. at 220 ˚C, the reaction was cooled to 70 ˚C and removed from the heating mantle. The NPs were precipitated out by adding ~75 mL hexane/isopropanol (v/v 1/9) and separated by centrifuging at 9,000 rpm for 8 min. The

precipitate was washed once more with 75 mL hexane/isopropanol (v/v 1/9) and then with 75 mL hexane/ethanol (v/v 1/9). The NPs were redispersed in hexane for further uses.

To make other varying compositions of Au:Pd NPs, the amount of precursors was adjusted accordingly. To make $Au_{24}Pd_{76}$, 0.035 g of $HAuCl_4$ and 0.082 g $Pd(acac)_2$ was used. To make $Au_{84}Pd_{16}$, 0.100 g of $HAuCl_4$ and 0.015 g $Pd(acac)_2$ was used. To make $Au_{40}Pd_{60}$, 0.060 g of $HAuCl_4$ and 0.07 g $Pd(acac)_2$ was used.

Synthesis of Pd NPs. Pd NPs were synthesized through adaption of a previously published synthesis.[2] 0.150 g of $Pd(acac)_2$ was added to 15 mL of oleylamine in a reaction flask and degassed with nitrogen or argon at 60 ˚C for a half hour (stirring at 800 rpm). Then, the temperature was lowered to 40 ˚C and 300 mg of borane *tert*-butylamine dispersed in 4 mL of oleylamine was added quickly to the reaction flask. Then, the temperature was raised to 90 ˚C (3-5 ˚C/min) and allowed to sit for 1 h. The workup procedure was the same as what was described in the synthesis of AuPd NPs. The NPs were redispersed in hexane for further uses.

Synthesis of AgPd and CuPd NPs. Pd NPs were used as seeds to synthesize AgPd and CuPd NPs. 0.3 mmol $Cu(acac)_2$ or 0.5 mmol AgOAc was dispersed in 15 mL oleylamine and 0.32 mL oleic acid and degassed under N_2 flow at 60 ˚C for a half hour. Then 26 mg of Pd NPs in 1 mL of hexane was added. The reaction was slowly heated (2-3 ˚C/min) to 260 ˚C and stayed at this temperature for 1 h before being cooled to room temperature. The NPs were separated and washed as described in the synthesis of AuPd NPs, and dispersed in hexane for further use.

Synthesis of Au NPs. Au NPs were synthesized through adaptation of a previously published synthesis.[3] To synthesize 4 nm Au NPs, 0.1 g of $HAuCl_4$ was mixed with 10 mL tetralin and 10 mL oleylamine and magnetically stirred (800 rpm) under nitrogen atmosphere at 28 ˚C. A solution of 0.5 mmol borane *tert*-butylamine was made in 1 mL tetralin and 1 mL oleylamine and was injected into the precursor solution. The reaction proceeded for one hour. After the reaction, acetone was added to precipitate the Au NPs. The NPs were then washed two times with hexane/ethanol (v/v 1/9) and separated each time via centrifugation at 9,000 rpm for 8 min. The NPs were dispersed in hexane for further use.

NP Loading on Carbon Support

Each group of the prepared NPs was loaded on carbon in similar manners. 60 mg of Ketjen Black EC300J carbon (C) was suspended in 30 mL of hexane for 1 h through sonication. Then 20 mg of NPs suspended in hexane were added dropwise to the C suspension and the mixture was

sonicated for another hour. The NPs were then washed with ethanol twice and separated by centrifugation at 7,000 rpm for 8 min. The C-NPs sample was dried in air and then added to 40 mL of acetic acid (AA) in a reaction flask. Under nitrogen blanket, the acetic acid suspension of C-NPs was heated to 70 ˚C overnight and cooled to room temperature. The C-NPs was washed one time with pure ethanol and then twice more with hexane/ethanol (v/v 1/9) (separated each time by centrifugation at 9,000 rpm for 8 mins) before being dried again in air.

Hydrogenation/Tandem Hydrogenation Reaction Conditions

In a typical hydrogenation reaction set-up, catalyst (AA-washed C-NPs) was added to a crimp-seal capped vial with a stir bar and then sealed. The vial and catalyst were vacuumed for 5-10 minutes. Next, 3 mmol of ethyl levulinate (EL) and 3 mmol of octylamine, as well as 35 μL of mesitylene as an internal standard, were added to the flask and the catalyst was mixed in the reactants. Then a H_2 balloon collected from either a pure H_2 cylinder or from a previous AB methanolysis reaction was connected to the reaction system via a needle. The vial was put in an oil bath set for 85 ˚C (stirring at 400 rpm). After the reaction, the product could be diluted with $CDCl_3$ and the catalyst was filtered for direct nuclear magnetic resonance (NMR) analysis.

To test catalyst stability of C-$Au_{66}Pd_{34}$, instead of $CDCl_3$, methanol was added to the catalyst/products of the model reaction of 3 mmol octylamine and 3 mmol ethyl levulinate after the catalyst reacted with the reactants for 12 h. The catalyst was centrifuged out (7,000 rpm for 8 min) and dried in air. This process was repeated nine times with the same catalyst. After the fifth and the tenth reaction cycle, the catalyst was analyzed by TEM. The catalyst was also analyzed by ICP-AES analysis to determine ratio of Au:Pd and metal loading.

Characterization

Samples for transmission electron microscopy (TEM) and high-resolution TEM (HR-TEM) analyses were prepared by depositing a single drop of diluted NP dispersion/suspension on amorphous-carbon-coated copper grids. Images were obtained by a JEOL 2100 TEM (200 kV). X-ray powder diffraction (XRD) patterns of the samples were collected on a Bruker AXS D8-Advanced diffractometer with Cu Kα radiation (λ = 1.5406 Å).

NP compositions were measured by inductively coupled plasma−atomic emission spectroscopy (ICP−AES). For ICP−AES analyses, the dried NPs were dissolved in warm aqua regia (~70 °C, two hours) to ensure the complete dissolution of metal into the acid. The solution

was then diluted with 2% HNO_3 solution. The measurements were carried out on a JY2000 Ultrace ICP−AES equipped with a JY-AS 421 auto sampler and 2400 g/mm holographic grating.

NMR spectra were recorded using a Bruker Avance III Ultra-Shield Spectrometer (400 MHz for ^{1}H, 100 MHz for ^{13}C) at 296 K. Chemical shifts are reported in ppm relative to the residual solvent signal ($CDCl_3$: 7.26 ppm (^{1}H), 77.16 ppm (^{13}C)). Routine determination of product amounts was done using mesitylene as the internal standard. Isolated yields were determined using flash column chromatography through silica gel, eluting with 7:3 (v:v) hexane:ethyl acetate and 3:7 (v:v) hexane:ethyl acetate.

X-ray photoelectron spectroscopy (XPS) measurements were taken on a Thermo Scientific K-Alpha^{+} instrument using Avantage software. Spectra were acquired using an aluminum anode (Al Kα = 1486.6 eV) operating with a spot size of 200 μm. Survey scans were measured at a pass energy of 200 eV and region scans at a pass energy of 20 eV.

Figures and Tables

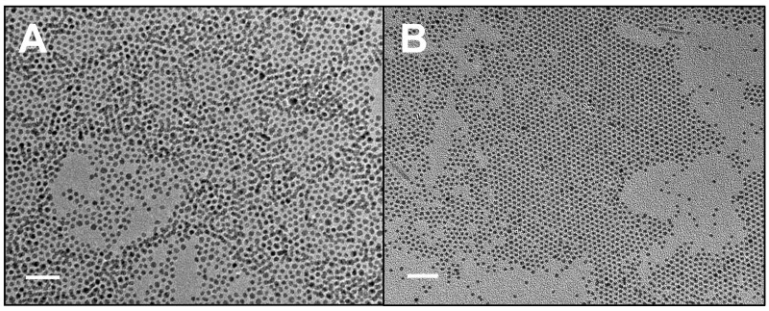

Figure S1. TEM images of as-synthesized (A) 4.5 nm Pd NPs and (B) 4 nm Au NPs. Scale bar = 20 nm.

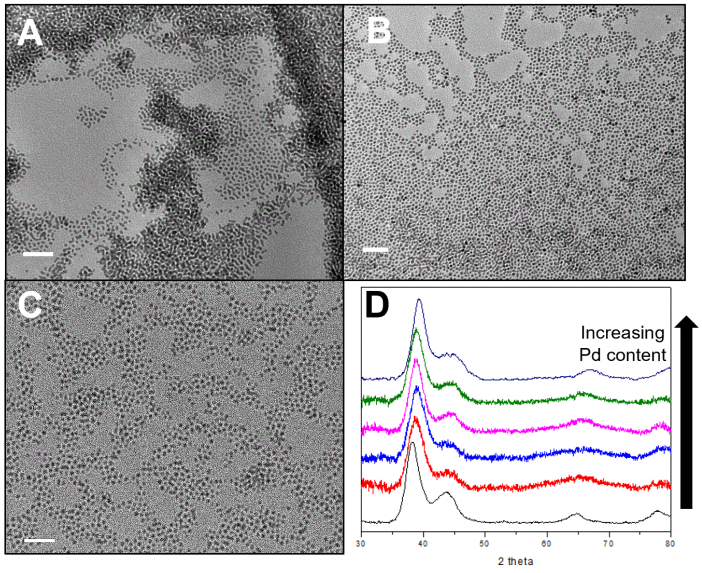

Figure S2. TEM images of 4 nm (A) $Au_{84}Pd_{12}$, (B) $Au_{40}Pd_{60}$, and (C) $Au_{24}Pd_{76}$. XRD patterns of (D) as-synthesized Au (bottom), Pd (top), and bimetallic alloys with increasing Pd content from bottom to top. Scale bar = 20 nm.

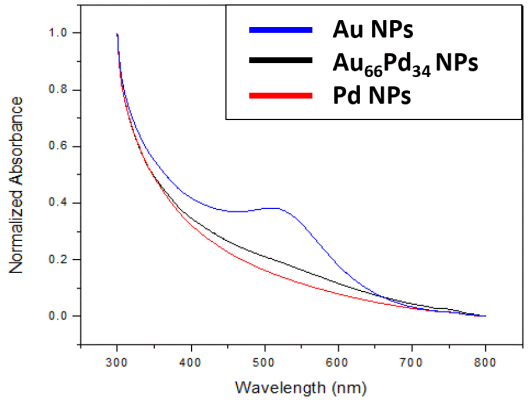

Figure S3. Normalized absorbance of as-synthesized 4 nm Au, $Au_{66}Pd_{34}$, and Pd NPs.

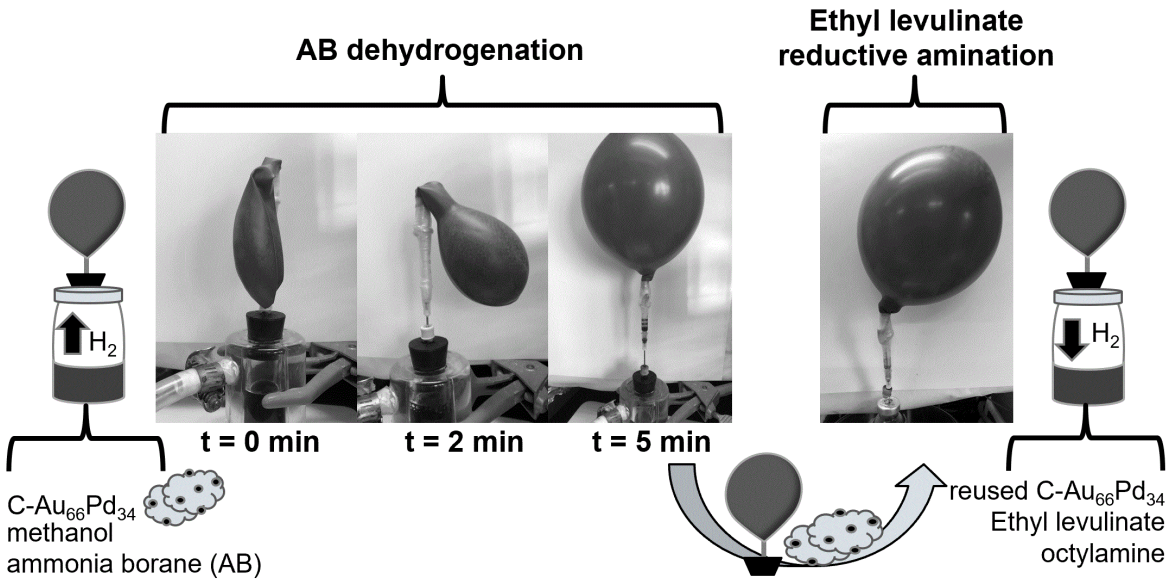

Figure S4. Hydrogen generated through AB methanolysis (left) was collected in a balloon and used in the reductive amination of EL (right). Reaction condition for AB hydrolysis: 25 ˚C, 9 mmol AB, 0.5 mol% C-$Au_{66}Pd_{34}$, 10 mL methanol. Reaction condition for EL reductive amination: 85 ˚C, 3 mmol EL, 3 mmol octylamine, 0.3 mol% C-$Au_{66}Pd_{34}$.

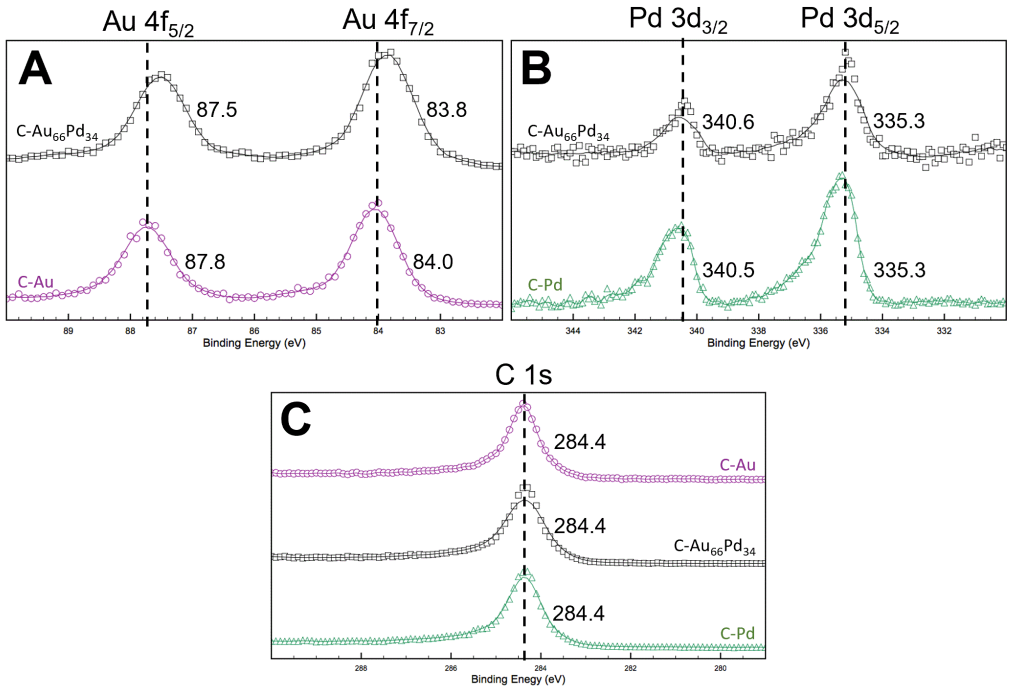

Figure S5. XPS spectra of C-Au and C-Pd catalysts compared with C-$Au_{66}Pd_{34}$ with detailed region scans, for (A) Au 4f spectral region, (B) Pd 3d spectral region, and (C) C 1s spectral region.

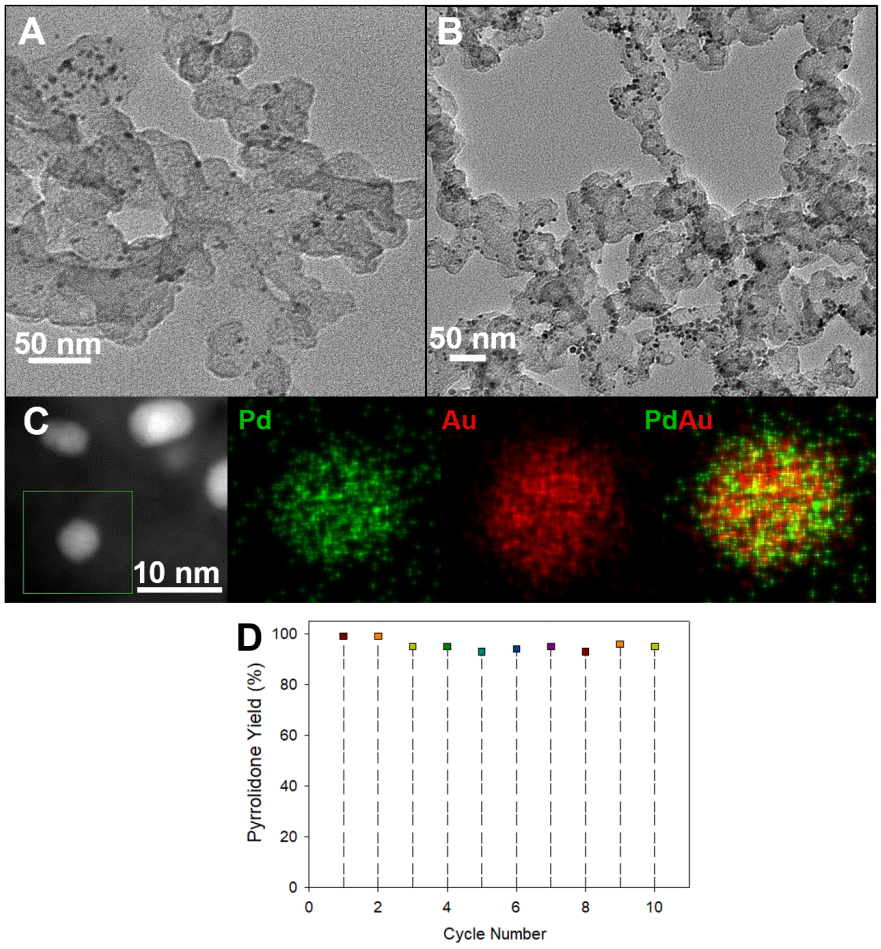

Figure S6. (A) TEM image of 15 wt% C-$Au_{66}Pd_{34}$ after five cycles of the reductive amination of EL, (B) TEM image of the 15 wt % C-$Au_{66}Pd_{34}$ after ten cycles of the reductive amination of EL, (C) HAADF-STEM image of the C-$Au_{66}Pd_{34}$ NPs and STEM-EELS elemental mapping of a selected NP to show Pd (green) and Au (red) distribution within the NP after five cycles of the reductive amination of EL, and (D) pyrrolidone yield of the reductive amination of EL determined using NMR with mesitylene as the internal standard after 10 reaction cycles.

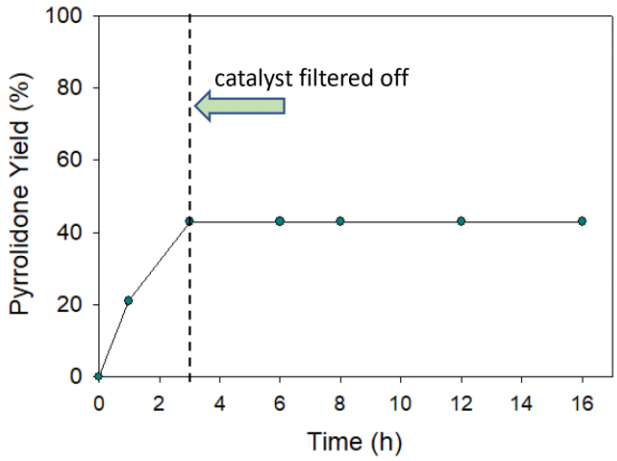

Figure S7. Reductive amination of ethyl levulinate (3 mmol) with octylamine (3 mmol) with 0.3 mol% C-$Au_{66}Pd_{34}$ as catalyst in toluene at 85°C with an H_2 balloon. The catalyst was filtered after 3 h and the reaction proceeded in toluene as the solvent with an H_2 balloon.

Table S1. C-$Au_{66}Pd_{34}$ tested under different reaction conditions for reacting ethyl levulinate with aliphatic amines to form pyrrolidone. The top entry is highlighted in the main text.

Catalyst	*Solvent*	*Reaction Conditions*	*Yield, time*
C-$Au_{66}Pd_{34}$	**None**	**1 atm H_2, 85 ˚C, octylamine**	**99%, 12 h**
C-$Au_{66}Pd_{34}$	None	1 atm H_2, 50 ˚C, octylamine	60%, 16 h
C-$Au_{66}Pd_{34}$	None	1 atm H_2, 25 ˚C, octylamine	35%, 48 h
C-$Au_{66}Pd_{34}$	xylene	1 atm H_2, 85 ˚C, octylamine	97%, 12 h
C-$Au_{66}Pd_{34}$	toluene	1 atm H_2, 85 ˚C, octylamine	93%, 12 h
C-$Au_{66}Pd_{34}$	DMSO	1 atm H_2, 85 ˚C, octylamine	0%, 18 h
C-$Au_{66}Pd_{34}$	water	1 atm H_2, 80 ˚C, butylamine	0%, 12 h
C-$Au_{66}Pd_{34}$ (in air for 1 year)	None	1 atm H_2, 85 ˚C, octylamine	98%, 12 h

Table S2. Different Pd-catalyzed reaction between ethyl levulinate and octylamine under 1 atm H_2 and at 85 ˚C. NP sizes are around 4 nm and total metal loadings are at 0.3 mol%.

Catalyst	*Yield, Time*
C-$Au_{66}Pd_{34}$	99%, 12 h
C-Pd	50%, 16 h
C-$Cu_{52}Pd_{48}$	37%, 16 h
C-$Ag_{48}Pd_{52}$	75%, 16 h

Table S3. Different catalysts and model reaction conditions used to test reductive amination of ethyl levulinate for the formation of pyrrolidone.

Catalyst	*TOF (h^{-1})*	*Reaction Conditions*	*Yield, Time*	*Reference*
C-$Au_{66}Pd_{34}$	200	1 atm H_2, 85 ˚C, octylamine	99%, 12 h	this work
Pt/TiO_2	733	10 atm H_2, 120 ˚C, aniline	98%, 6 h	[4]
Pt/TiO_2-NT	390	10 atm H_2, 120 ˚C, nitrobenzene	92%, 48 h	[5]
Ru-PP/CNTs	-	30 atm H_2, 120 ˚C, octylamine, and THF solvent	93%, 24 h	[6]

Table S4. Different catalysts and model reaction conditions used to test reductive amination of levulinic acid for the formation of pyrrolidone.

Catalyst	*TOF (h^{-1})*	*Reaction Conditions*	*Yield, Time*	*Reference*
Pd/ZrO_2	-	5 atm H_2, 90 ˚C, octylamine	97%, 12 h	[7]
Pd/C	-	5 atm H_2, 90 ˚C, octylamine	10%, 12 h	[7]
Au/ZrO_2	-	5 atm N_2, formic acid, 130 ˚C, benzylamine	98%, 12 h	[8]
Pt-MoOx/TiO_2	-	3 atm H_2, 100 ˚C, octylamine	99%, 20 h	[9]
Pt-MoO_x/TiO_2	-	7 atm H_2, 110 ˚C, n-octanenitrile	92%, 24 h	[10]
FeNi	-	50 atm H_2, continuous flow, phenethylamine and ethanol as solvent	92% conversion	[11]
Ru	-	Formic acid, homogenous catalyst, phosphine ligand, autogenous pressure from formic acid decomposition, 120˚C, cyclohexylamine	79%, 12 h	[12]
Ir	-	Homogenous catalyst, formic acid, autogenous pressure from formic acid decomposition, 80 ˚C, benzylamine	86%, 4 h	[13]

Product Characterization Data

Entry 1. 5-methyl-1-octylpyrrolidin-2-one ($C_{13}H_{25}NO$):[9]

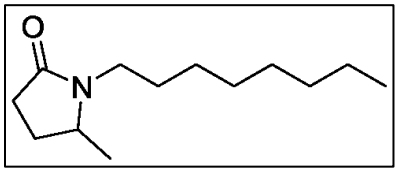

^{1}H NMR (400 MHz, $CDCl_3$) δ (ppm): 3.66-3.56 (m, 1H), 3.54-3.44 (m, 1H), 2.88-2.77 (m, 1H), 2.37-2.18 (m, 2H), 2.16-2.04 (m, 1H), 1.55-1.29 (m, 3H), 1.26-1.14 (m, 10H), 1.135-1.09 (d, *J*= 6.86Hz, 3H), 0.82 (t, *J*=7.0Hz, 3H)
^{13}C NMR (100 MHz, $CDCl_3$) δ (ppm): 174.3, 53.0, 39.8, 31.6, 30.2, 29.1, 29.0, 27.2, 26.8, 26.6, 22.4, 19.6, 13.8

Entry 2. 1-pentyl-5-methylpyrrolidin-2-one ($C_{10}H_{19}NO$):[14]

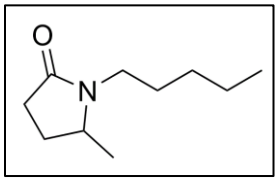

^{1}H NMR (400 MHz, $CDCl_3$) δ (ppm): 3.68-3.57 (m, 1H), 3.55-3.45 (m, 1H), 2.89-2.79 (m, 1H), 2.39-2.19 (m, 2H), 2.18-2.05 (m, 1H), 1.5-1.30 (m, 3H), 1.30-1.12 (m, 4H), 1.13 (d, *J*= 6.3Hz, 3H), 0.82 (t, *J*=6.9Hz, 3H)
^{13}C NMR (100 MHz, $CDCl_3$) δ (ppm): 174.5, 53.1, 39.9, 30.3, 29.1, 27.1, 26.8, 22.4, 19.7, 13.8

Entry 3. 1-hexyl-5-methylpyrrolidin-2-one ($C_{11}H_{21}NO$):[9]

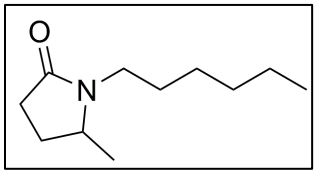

^{1}H NMR (400 MHz, $CDCl_3$) δ (ppm): 3.66-3.56 (m, 1H), 3.55-3.46 (m, 1H), 2.88-2.78 (m, 1H), 2.38-2.17 (m, 2H), 2.18-2.04 (m, 1H), 1.5-1.308 (m, 3H), 1.20 (s, 6H), 1.12 (d, *J*= 6.3Hz, 3H), 0.79 (t, *J*=6.6Hz, 3H)
^{13}C NMR (100 MHz, $CDCl_3$) δ (ppm): 174.5, 53.1, 39.9, 31.5, 30.3, 27.3, 26.7, 26.6, 22.5, 19.7, 13.9

Entry 4. 1-butyl-5-methylpyrrolidin-2-one ($C_9H_{17}NO$):[14]

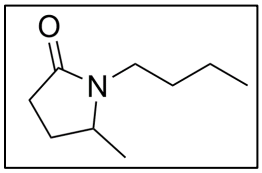

^{1}H NMR (400 MHz, $CDCl_3$) δ (ppm): 3.73-3.64 (m, 1H), 3.63-3.54 (m, 1H), 2.97-2.86 (m, 1H), 2.46-2.27 (m, 2H), 2.23-2.12 (m, 1H), 1.62-1.37 (m, 3H), 1.37-1.23 (m, 2H), 1.20 (d, *J*= 6.2Hz, 3H), 0.82 (t, *J*=7.3Hz, 3H)
^{13}C NMR (100 MHz, $CDCl_3$) δ (ppm): 174.7, 53.2, 39.7, 30.4, 29.5, 26.8, 20.2, 19.8, 13.8

Entry 5. 1-dodecyl-5-methylpyrrolidin-2-one ($C_{17}H_{33}NO$):[13]

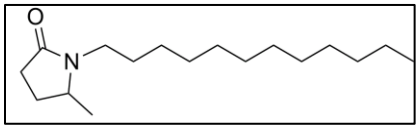

^{1}H NMR (400 MHz, $CDCl_3$) δ (ppm): 3.72-3.64 (m, 1H), 3.62-3.53 (m, 1H), 2.95-2.85 (m, 1H), 2.46-2.26 (m, 2H), 2.23-2.12 (m, 1H), 1.63-1.37 (m, 3H), 1.31-1.22 (m, 18H), 1.19 (d, *J*= 6.29Hz, 3H), 0.87 (t, *J*=6.6Hz, 3H)
^{13}C NMR (100 MHz, $CDCl_3$) δ (ppm): 174.6, 53.2, 40.0, 31.9, 30.4, 29.64, 29.63, 29.58, 29.56, 29.37, 29.35, 27.4, 27.0, 26.8, 22.7, 19.8

Entry 6. 1-hexadecyl-5-methylpyrrolidin-2-one ($C_{21}H_{41}NO$):

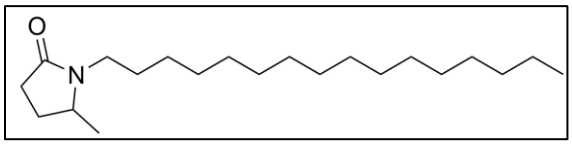

^{1}H NMR (400 MHz, $CDCl_3$) δ (ppm): 3.74-3.64 (m, 1H), 3.63-3.53 (m, 1H), 2.95-2.85 (m, 1H), 2.47-2.26 (m, 2H), 2.23-2.11 (m, 1H), 1.62-1.37 (m, 3H), 1.38-1.22 (m, 26H), 1.2 (d, *J*= 6.26Hz, 3H), 0.88 (t, *J*=6.9Hz, 3H)
^{13}C NMR (100 MHz, $CDCl_3$) δ (ppm): 174.6, 53.2, 40.0, 31.9, 30.4, 29.7, 29.67, 29.65, 29.59, 29.56, 29.37, 27.45, 27.0, 26.8, 22.7, 26.8, 22.7, 19.8, 14.1

Entry 7. 5-methyl-1-octadecylpyrrolidin-2-one ($C_{23}H_{45}NO$):

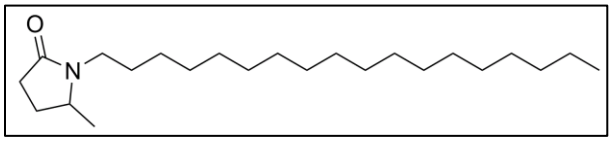

^{1}H NMR (400 MHz, $CDCl_3$) δ (ppm): 3.76-3.65 (m, 1H), 3.64-3.55 (m, 1H), 2.98-2.87 (m, 1H), 2.48-2.29 (m, 2H), 2.24-2.14 (m, 1H), 1.65-1.38 (m, 3H), 1.36-1.23 (m, 30H), 1.2 (d, *J*= 6.42Hz, 3H), 0.88 (t, *J*=6.55Hz, 3H)
^{13}C NMR (100 MHz, $CDCl_3$) δ (ppm): 174.6, 53.2, 40.0, 31.9, 30.4, 29.71, 29.68, 29.61, 29.58, 29.38, 27.5, 27.0, 26.8, 22.7, 19.8, 14.1

Entry 8. 1-isopentyl-5-methylpyrrolidin-2-one ($C_{10}H_{19}NO$):[14]

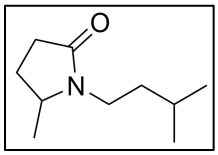

^{1}H NMR (400 MHz, $CDCl_3$) δ (ppm): 3.74-3.58 (m, 2H), 2.98-2.87 (m, 1H), 2.47-2.27 (m, 2H), 2.25-2.13 (m, 1H), 1.65-1.51 (m, 2H), 1.47-1.29 (m, 2H), 1.21 (d, *J*= 6.21Hz, 3H), 0.93 (d, *J*=6.97Hz, 6H)
^{13}C NMR (100 MHz, $CDCl_3$) δ (ppm): 174.5, 53.1, 38.3, 36.1, 30.4, 26.8, 26.1, 22.7, 22.3, 19.8

Entry 9. 1-(2-methoxyethyl)-5-methylpyrrolidin-2-one ($C_8H_{15}NO_2$):

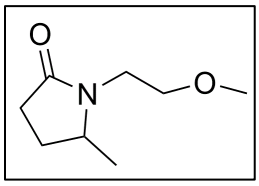

^{1}H NMR (400 MHz, $CDCl_3$) δ (ppm): 3.80-3.66 (m, 2H), 3.48-3.40 (m, 2H), 3.28 (s, 3H), 3.13-3.03 (m, 1H), 2.42-2.23 (m, 2H), 2.2-2.09 (m, 1H), 1.59-1.45 (m, 1H), 1.16 (d, *J*=6.17Hz, 3H)
^{13}C NMR (100 MHz, $CDCl_3$) δ (ppm): 175.0, 70.5, 58.7, 54.3, 39.7, 30.1, 26.8, 19.7

Entry 10. 1-(3-hydroxypropyl)-5-methylpyrrolidin-2-one ($C_8H_{15}NO_2$):

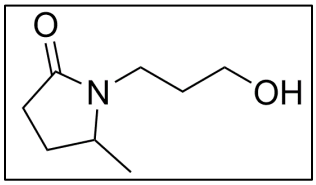

^{1}H NMR (400 MHz, $CDCl_3$) δ (ppm): 3.93 (s, br, 1H), 3.74-3.62 (m, 1H), 3.619-3.4 (m, 3H), 3.38-3.24 (m, 1H), 2.56-2.32 (m, 2H), 2.3-2.18 (m, 1H), 1.74-1.57 (m, 3H), 1.26 (d, *J*=6.41Hz, 3H)
^{13}C NMR (100 MHz, $CDCl_3$) δ (ppm): 176.6, 58.2, 54.5, 36.5, 30.45, 30.13, 27.1, 20.2

Entry 11. 1-cyclohexyl-5-methylpyrrolidin-2-one ($C_{11}H_{19}NO$):[9]

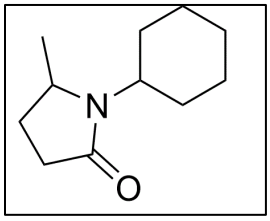

^{1}H NMR (400 MHz, $CDCl_3$) δ (ppm): 3.85-3.66 (m, 2H), 2.52-2.40 (m, 1H), 2.31-2.21 (m, 1H), 2.20-2.07 (m, 1H), 1.89-1.72 (m, 3H), 1.71-1.44 (m, 5H), 1.42-1.29 (m, 2H), 1.25 (d, *J*=6.15Hz, 3H), 1.19-1.06 (m, 1H)
^{13}C NMR (100 MHz, $CDCl_3$) δ (ppm): 174.5, 52.8, 52.5, 31.9, 30.4, 30.1, 27.5, 26.0, 25.9, 25.6, 22.5

Entry 12. 5-methyl-1-phenethylpyrrolidin-2-one ($C_{13}H_{17}NO$):[9]

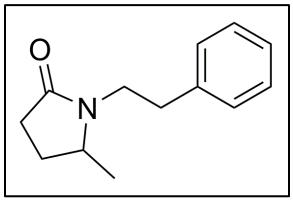

^{1}H NMR (400 MHz, $CDCl_3$) δ (ppm): 7.35-7.18 (m, 5H), 3.91-3.79 (m, 1H), 3.59-3.49 (m, 1H), 3.22-3.10 (m, 1H), 2.94-2.84 (m, 1H), 2.84-2.72 (m, 1H), 2.47-2.24 (m, 2H), 2.19-2.05 (m, 1H), 1.61-1.49 (m, 1H), 1.17 (d, *J*=6.37Hz, 3H)
^{13}C NMR (100 MHz, $CDCl_3$) δ (ppm): 174.8, 138.98, 128.75, 128.5, 126.4, 53.7, 41.7, 33.9, 30.3, 26.8, 19,75

Entry 13. 1-benzyl-5-methylpyrrolidin-2-one ($C_{12}H_{15}NO$):[9]

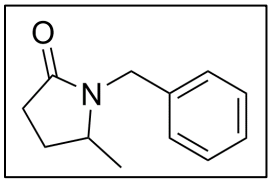

^{1}H NMR (400 MHz, $CDCl_3$) δ (ppm): 7.38-7.19 (m, 5H), 4.98 (d, *J*=15.6, 1H), 4.02 (d, 15.03, 1H), 3.59-3.48 (m, 1H), 2.59-2.34 (m, 2H), 2.23-2.10 (m, 1H), 1.67-1.55 (m, 1H), 1.18 (d, *J*=6.39Hz, 3H)
^{13}C NMR (100 MHz, $CDCl_3$) δ (ppm): 174.95, 136.9, 128.6, 127.99, 127.4, 52.8, 43.9, 30.3, 26.7, 19.6

Entry 14. 5-methyl-1-phenylpyrrolidin-2-one ($C_{11}H_{13}NO$):[13]

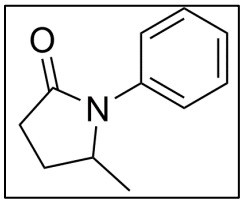

^{1}H NMR (400 MHz, $CDCl_3$) δ (ppm): 7.45-7.36 (m, 4H), 7.26-7.20 (m, 1H), 4.38-4.26 (m, 1H), 2.73-2.49 (m, 2H), 2.48-2.34 (m, 1H), 1.84-1.72 (m, 1H), 1.23 (d, *J*=6.14Hz, 3H)
^{13}C NMR (100 MHz, $CDCl_3$) δ (ppm): 174.2, 137.6, 129.0, 125.8, 124.1, 55.6, 31.4, 26.8, 20.2

Entry 16. 6-methyl-1-octylpiperidin-2-one ($C_{14}H_{27}NO$):[10]

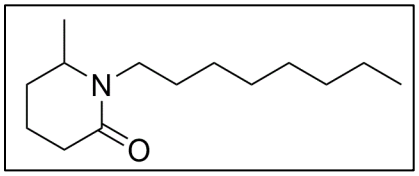

^{1}H NMR (400 MHz, $CDCl_3$) δ (ppm): 3.78-3.69 (m, 1H), 3.57-3.48 (m, 1H), 2.96-2.82 (m, 1H), 2.42-2.30 (m, 2H), 1.92-1.83 (m, 2H), 1.75-1.46 (m, 4H), 1.32-1.24 (m, 10H), 1.22 (d, *J*=6.55Hz, 3H), 0.87 (t, *J*=6.76Hz, 3H)
^{13}C NMR (100 MHz, $CDCl_3$) δ (ppm): 169.7, 51.8, 45.1, 32.2, 31.8, 30.2, 29.4, 29.3, 27.7, 27.1, 22.6, 19.9, 17.5, 14.1

NMR Spectra of Isolated Products

Entry 1. 5-methyl-1-octylpyrrolidin-2-one:

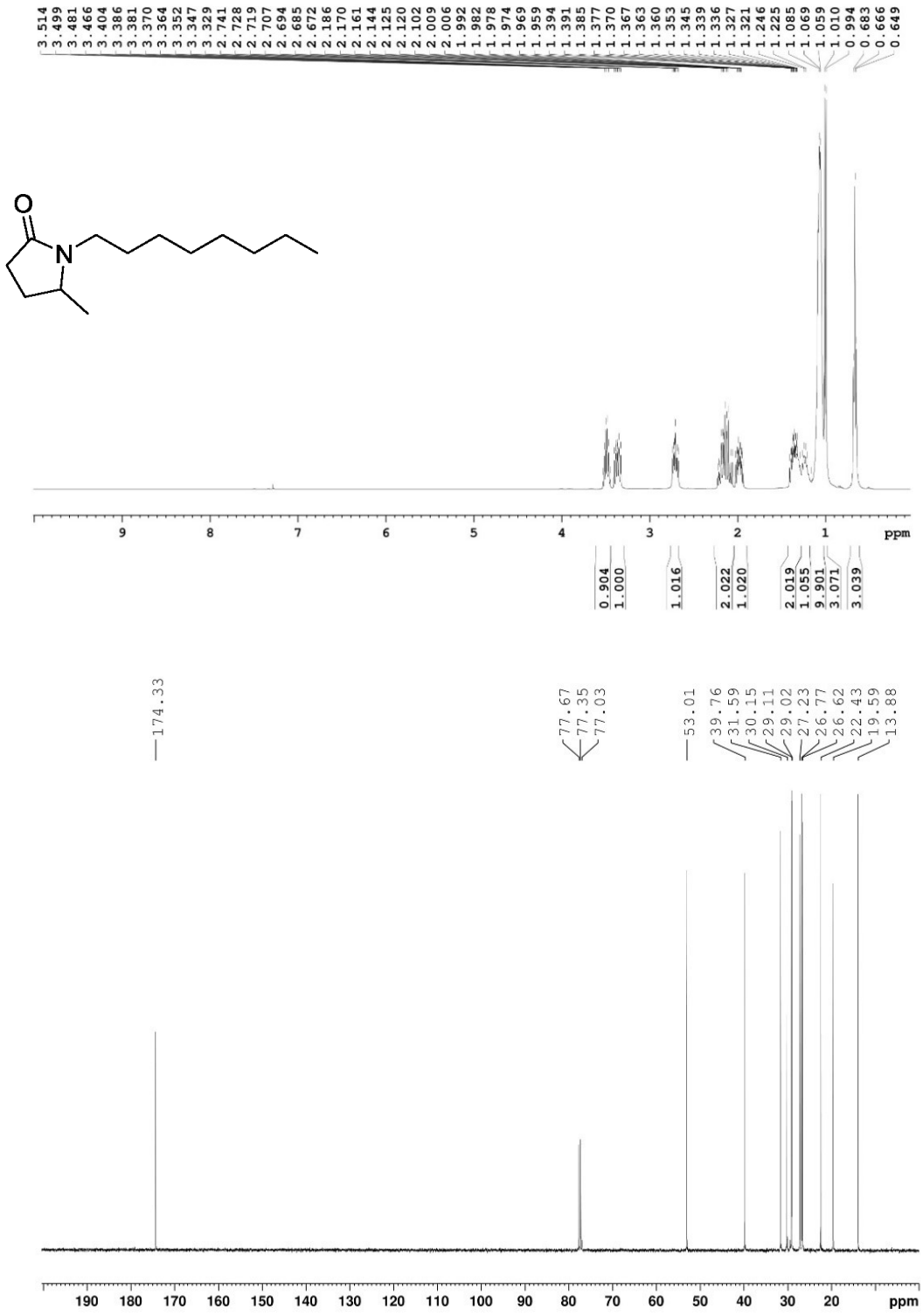

Entry 2. 1-pentyl-5-methylpyrrolidin-2-one:

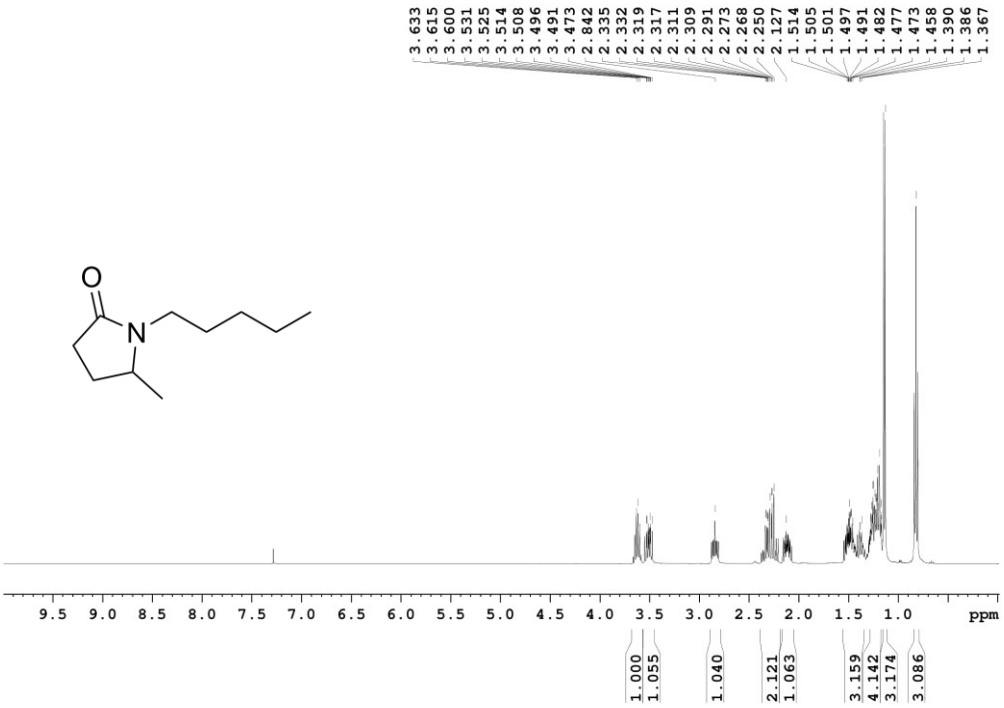

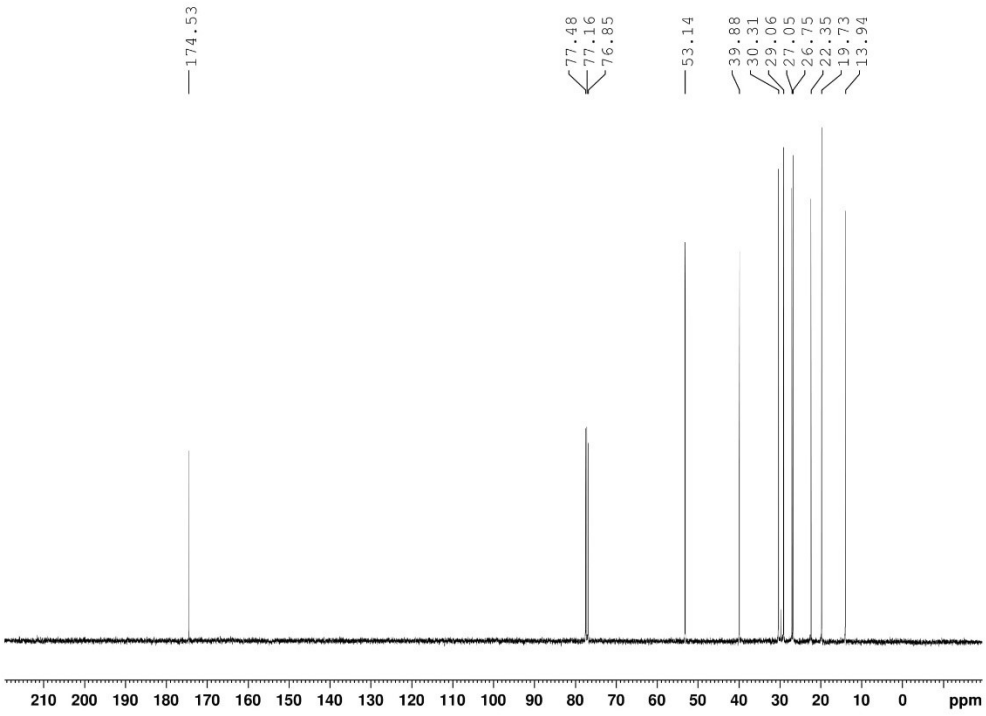

Entry 3. 1-hexyl-5-methylpyrrolidin-2-one:

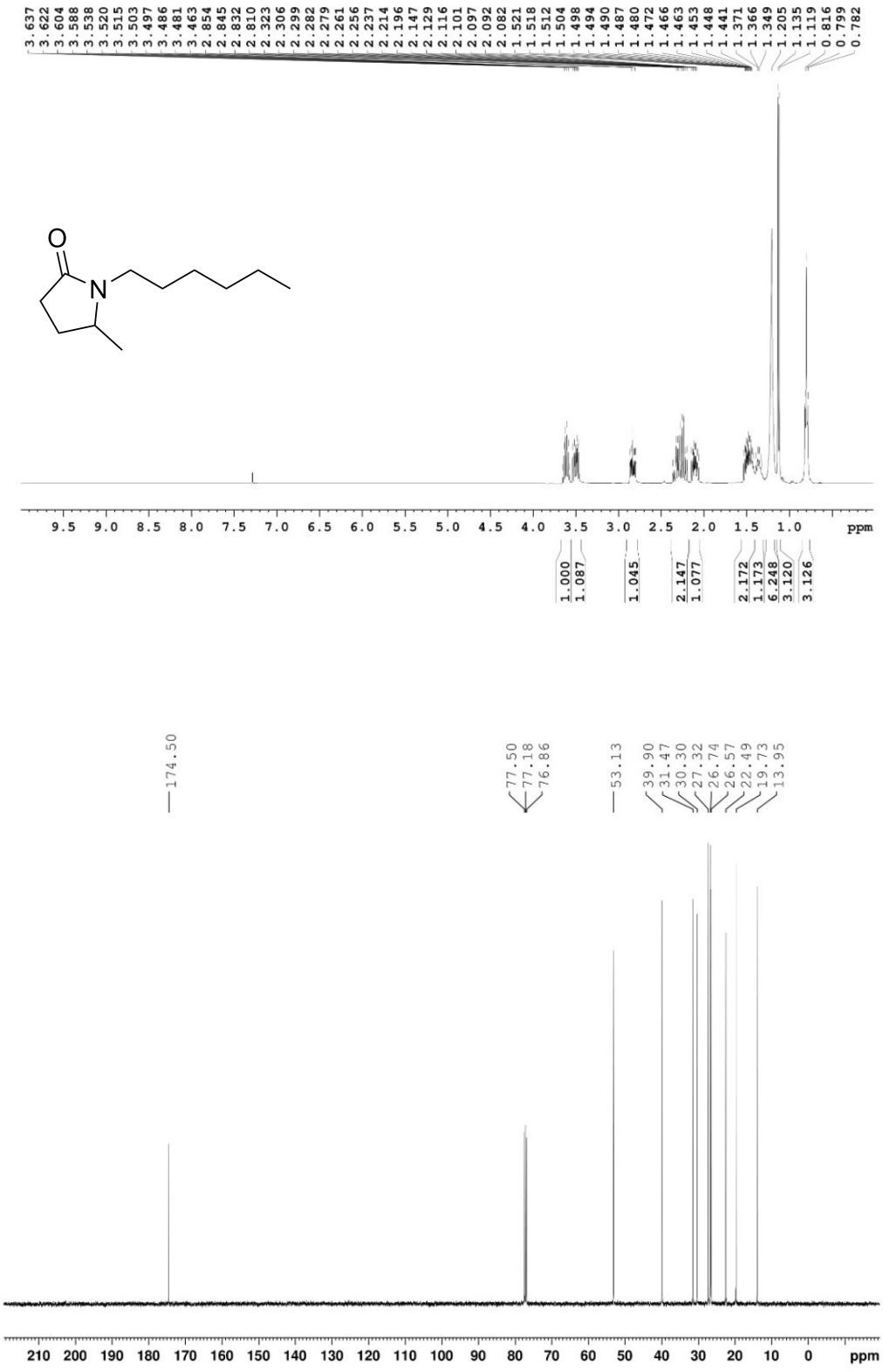

Entry 4. 1-butyl-5-methylpyrrolidin-2-one:

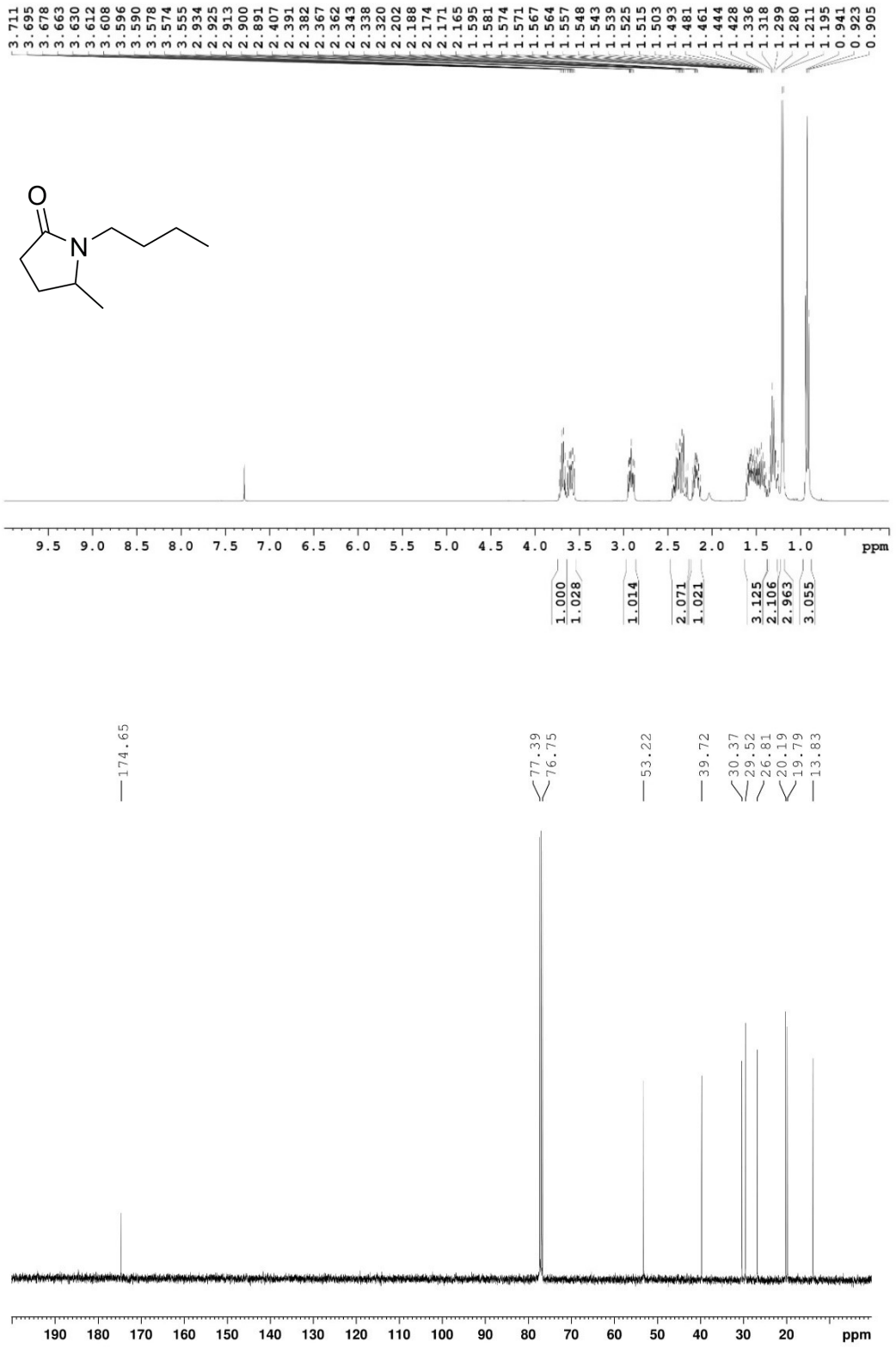

Entry 5. 1-dodecyl-5-methylpyrrolidin-2-one:

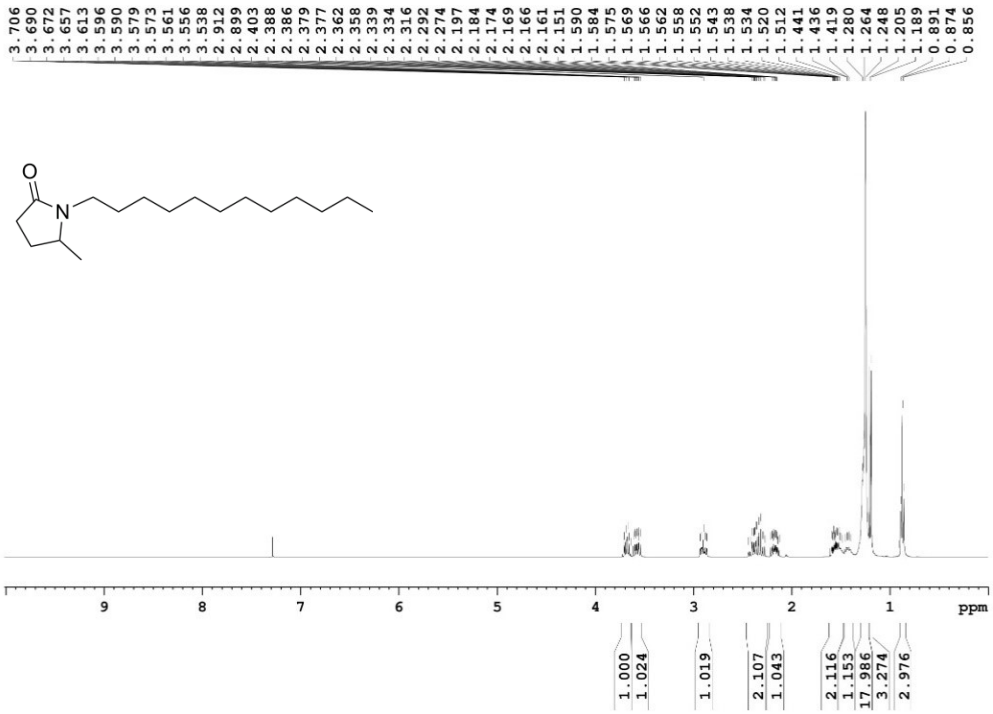

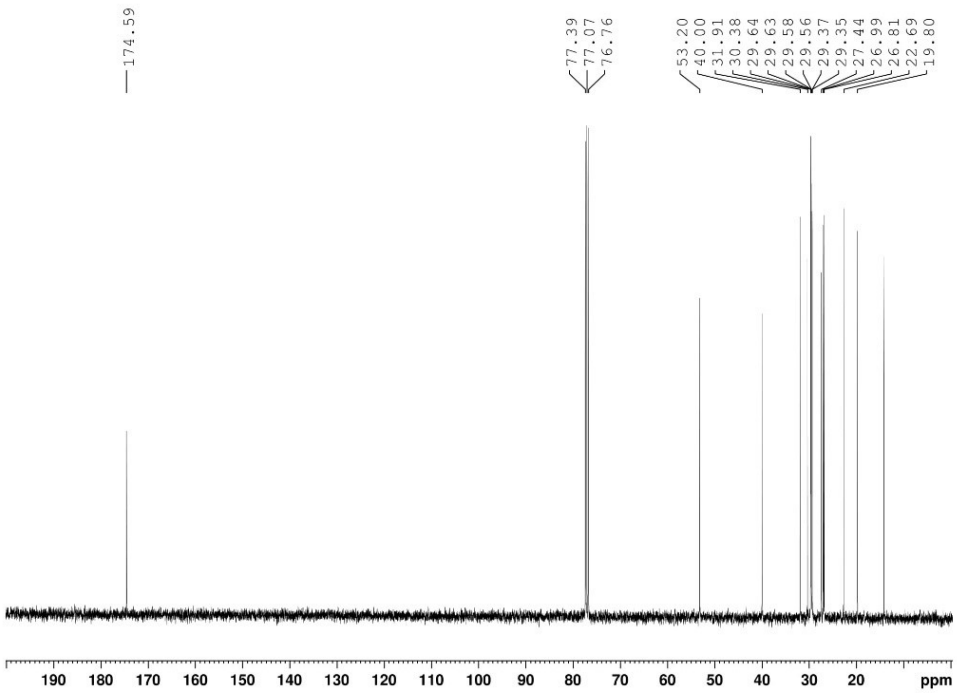

Entry 6. 1-hexadecyl-5-methylpyrrolidin-2-one:

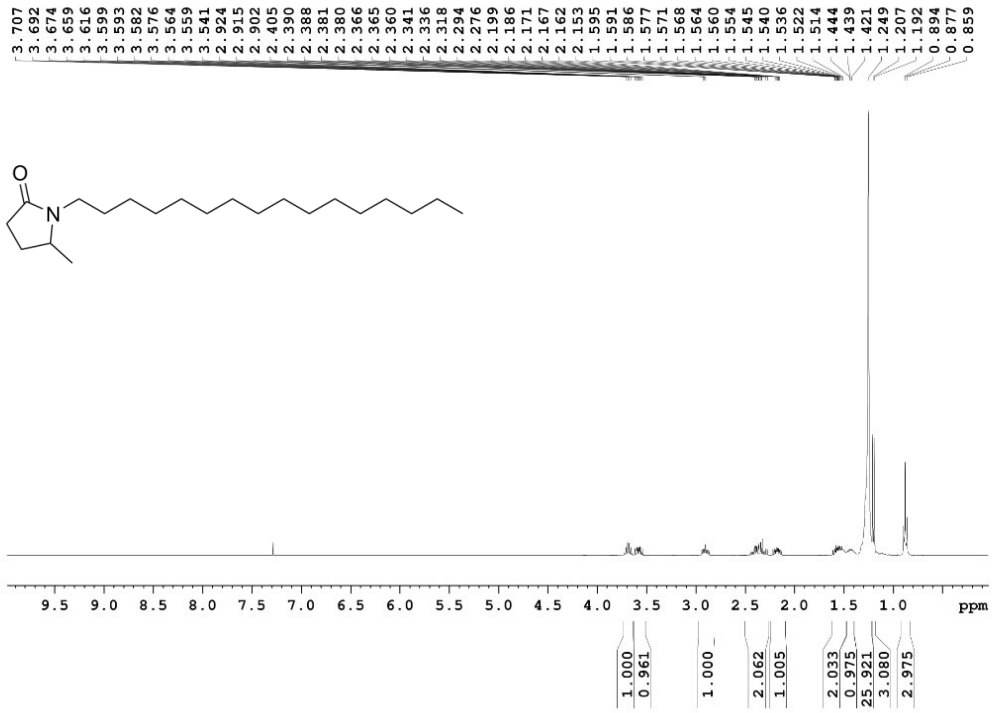

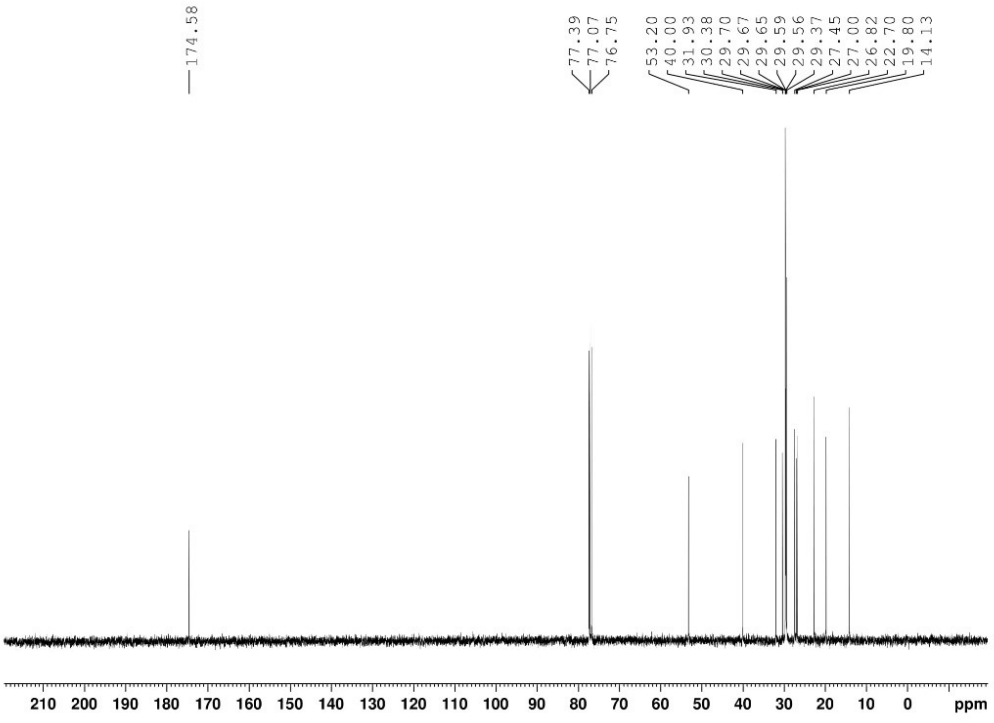

Entry 7. 5-methyl-1-octadecylpyrrolidin-2-one:

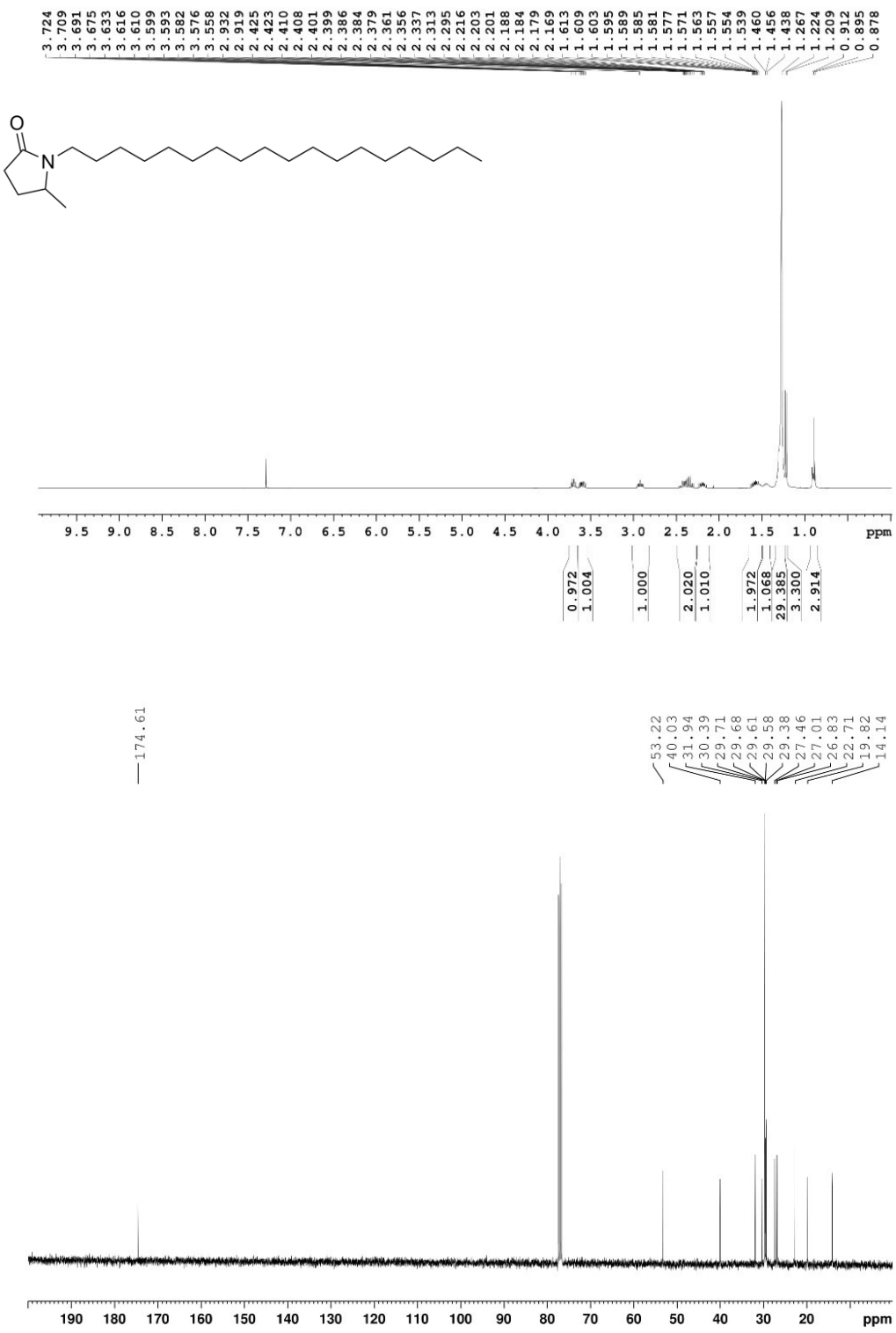

Entry 8. 1-isopentyl-5-methylpyrrolidin-2-one:

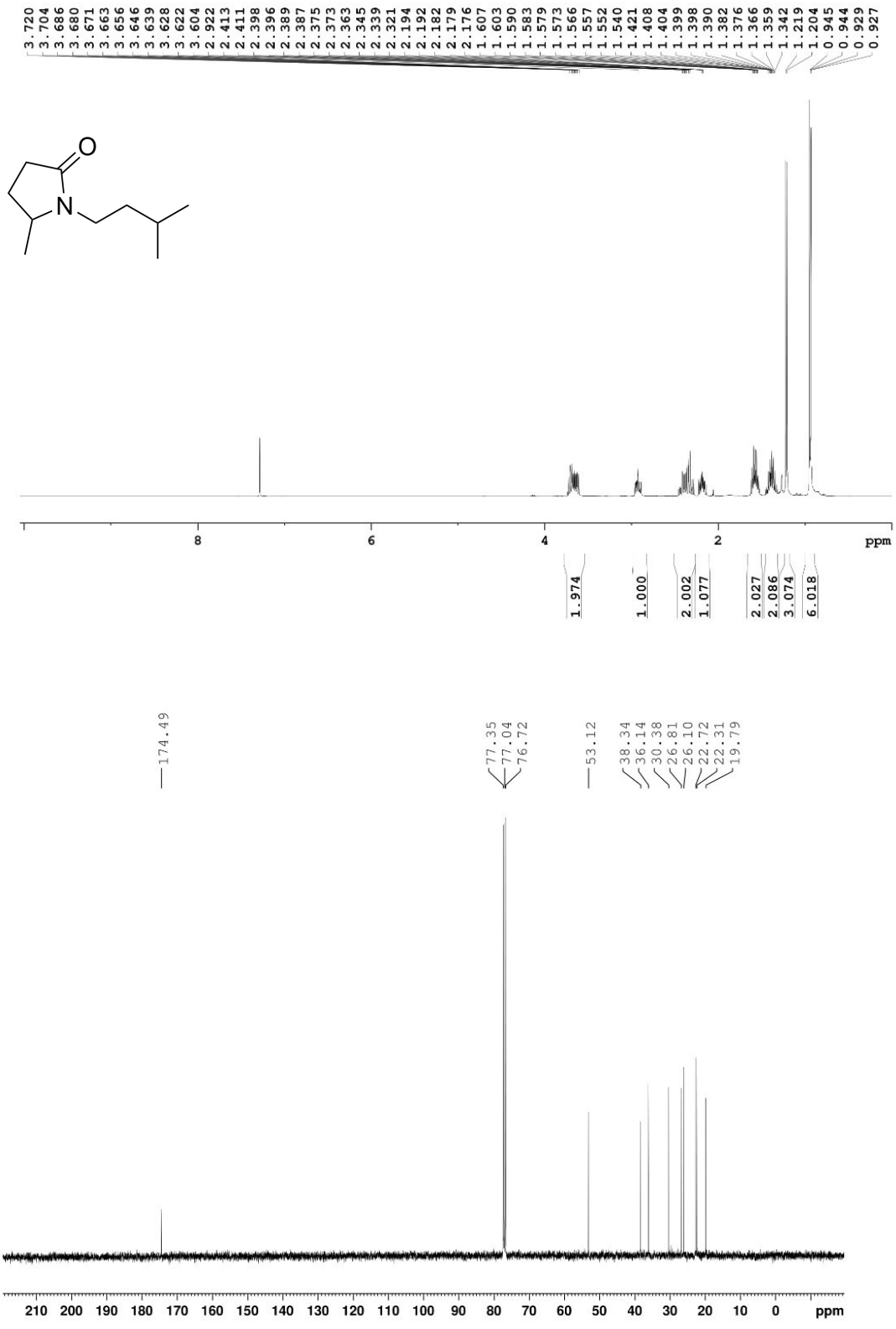

Entry 9. 1-(2-methoxyethyl)-5-methylpyrrolidin-2-one:

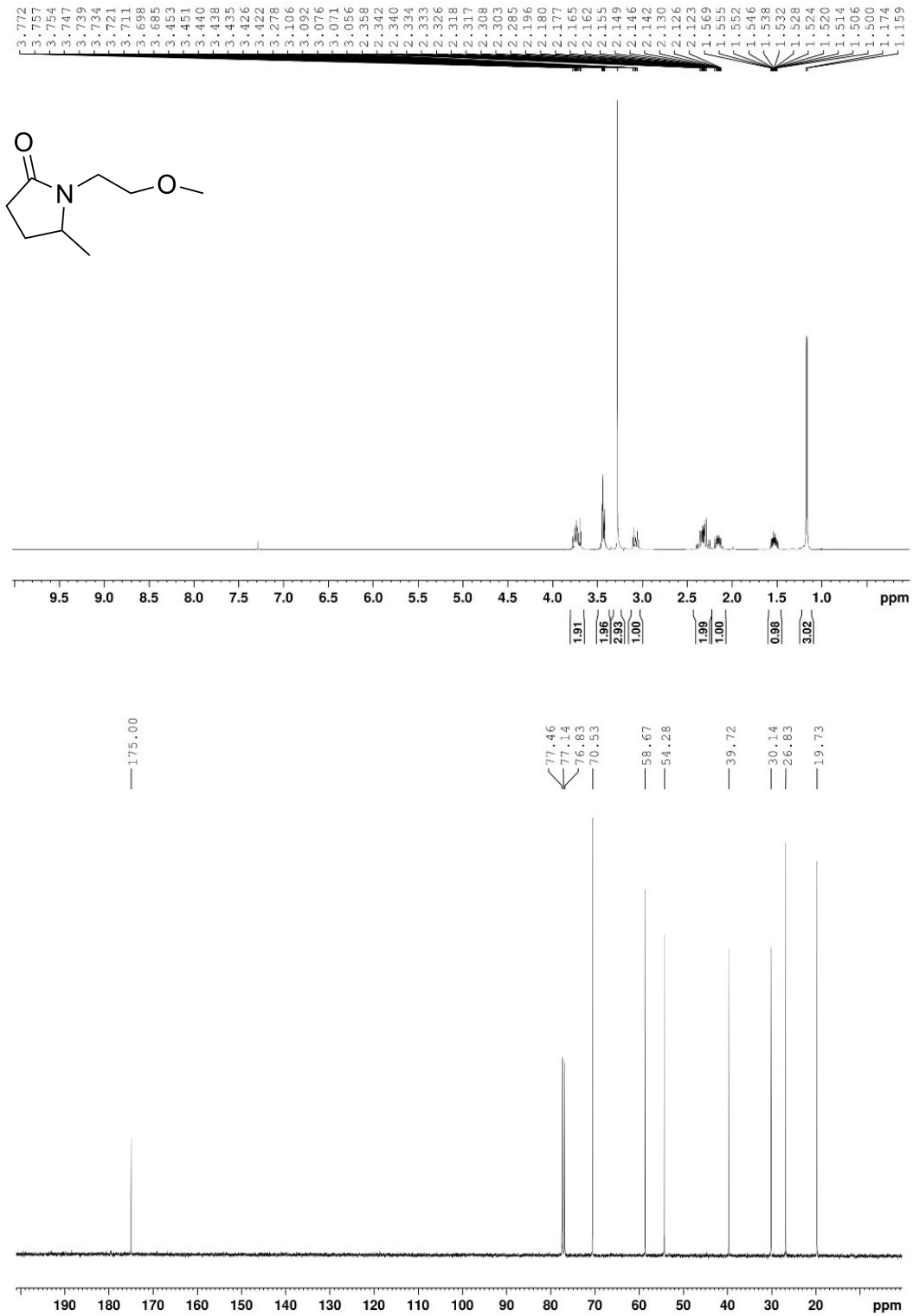

Entry 10. 1-(3-hydroxypropyl)-5-methylpyrrolidin-2-one:

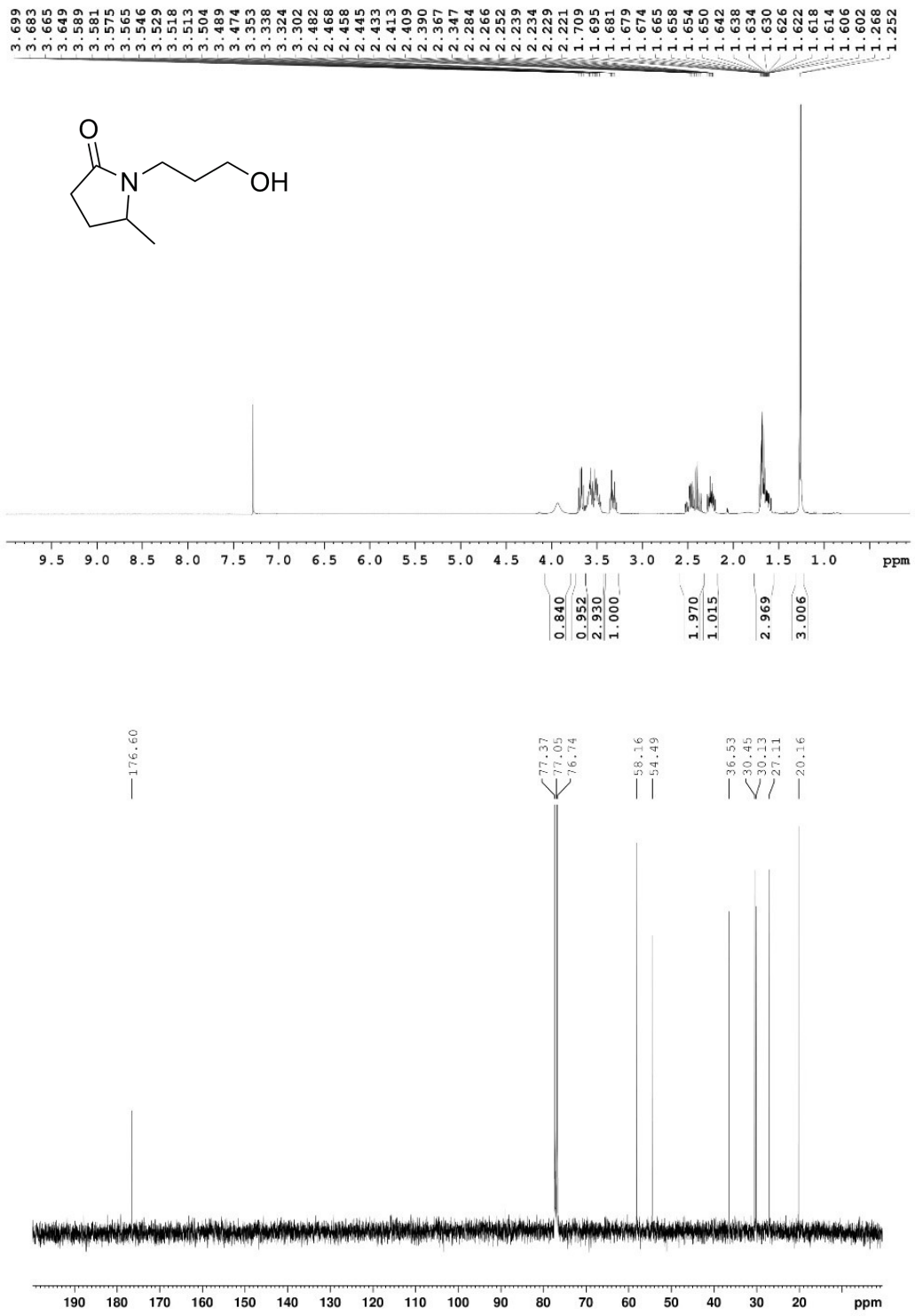

Entry 11. 1-cyclohexyl-5-methylpyrrolidin-2-one:

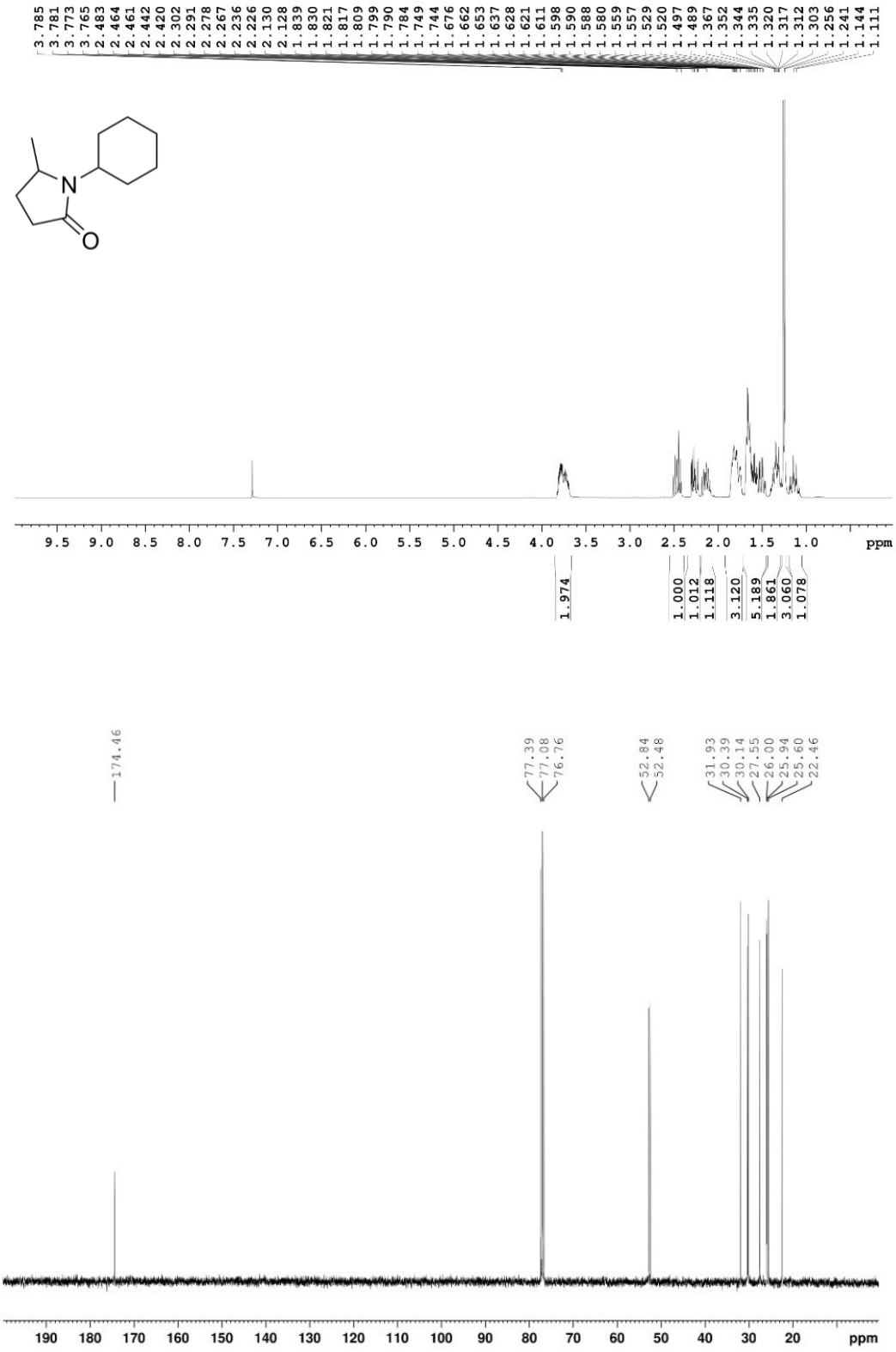

Entry 12. 5-methyl-1-phenethylpyrrolidin-2-one:

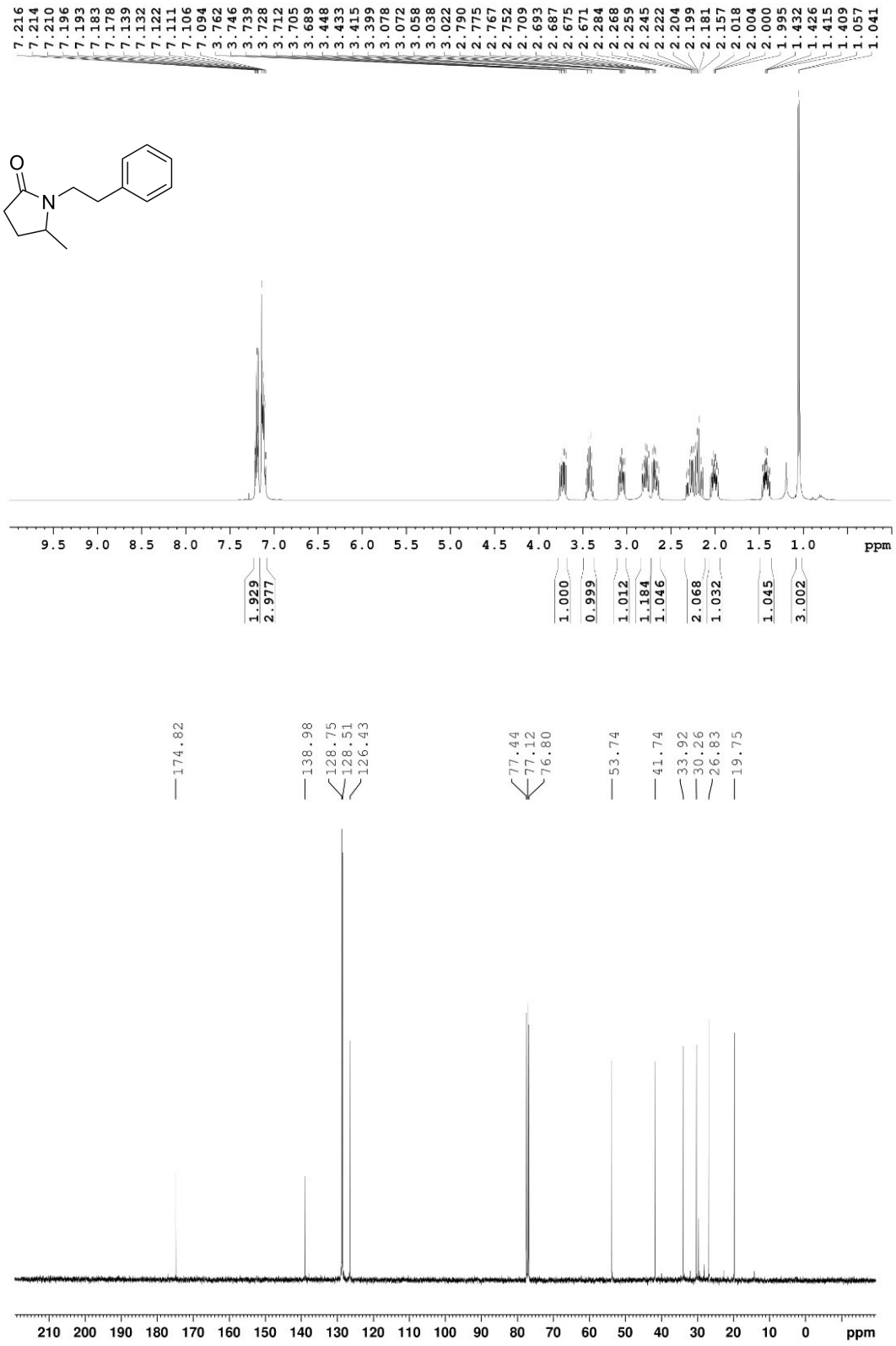

Entry 13. 1-benzyl-5-methylpyrrolidin-2-one:

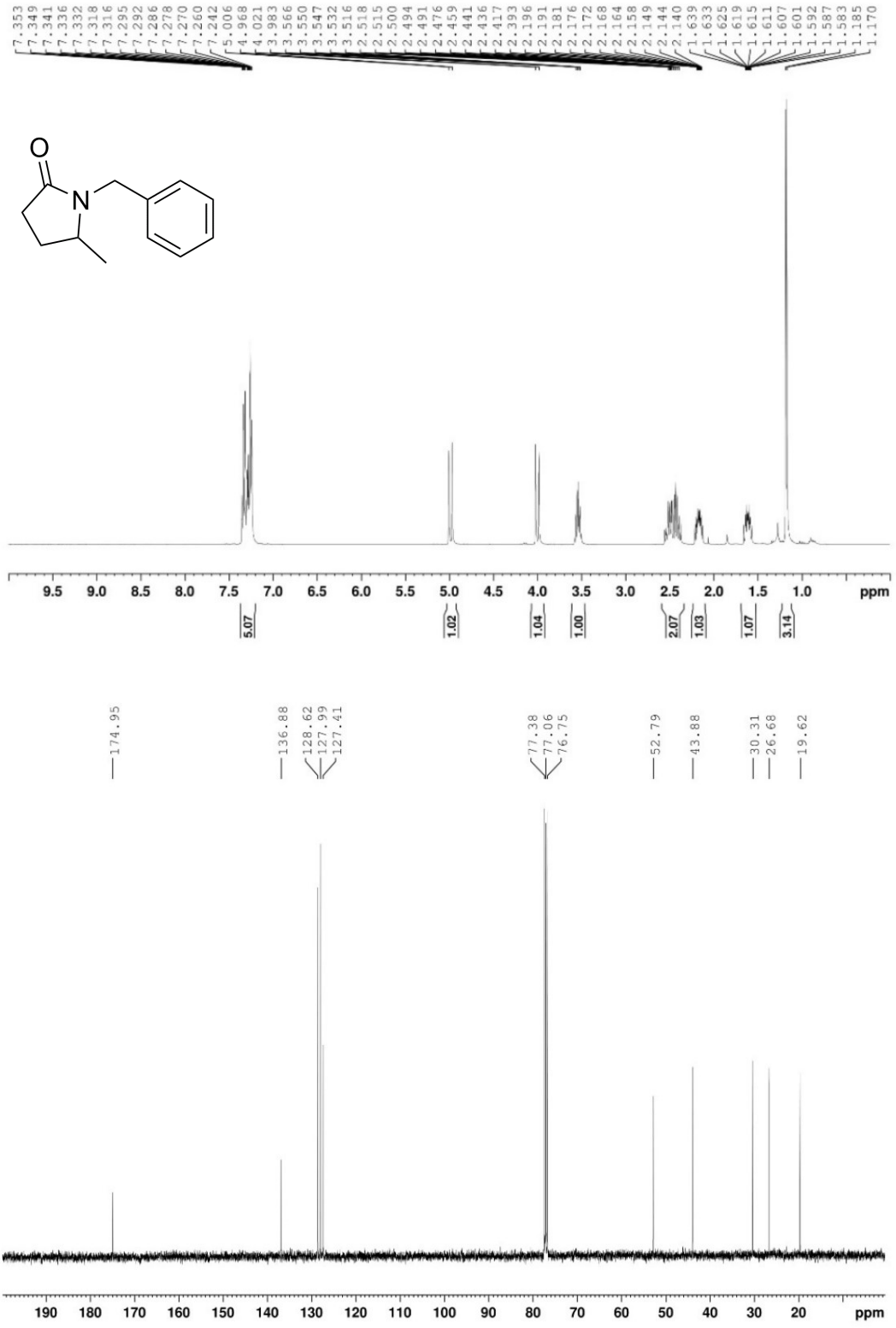

Entry 14. 5-methyl-1-phenylpyrrolidin-2-one:

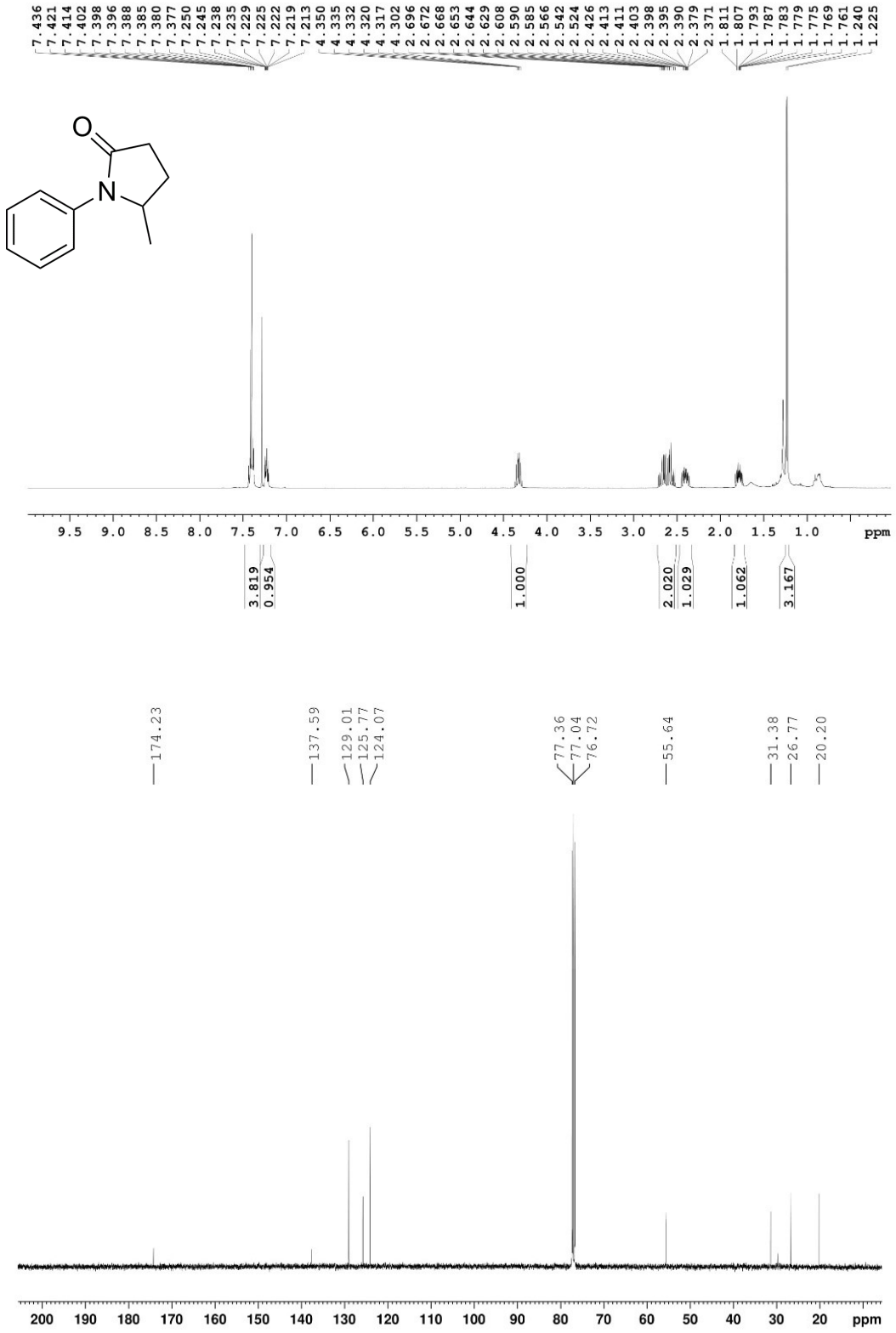

Entry 16. 6-methyl-1-octylpiperidin-2-one

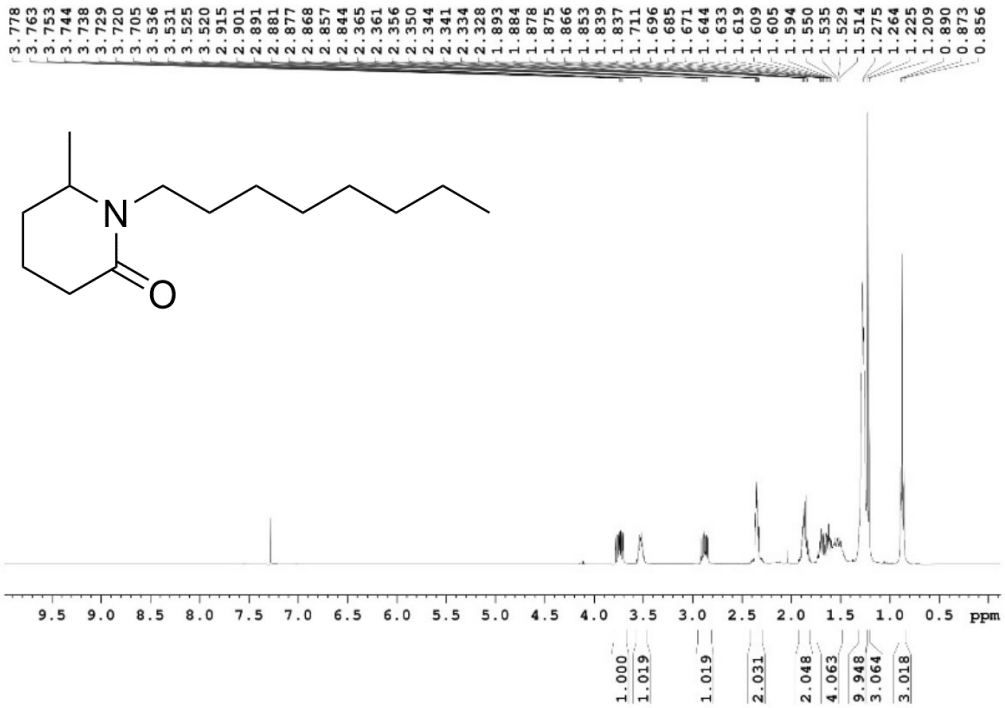

:

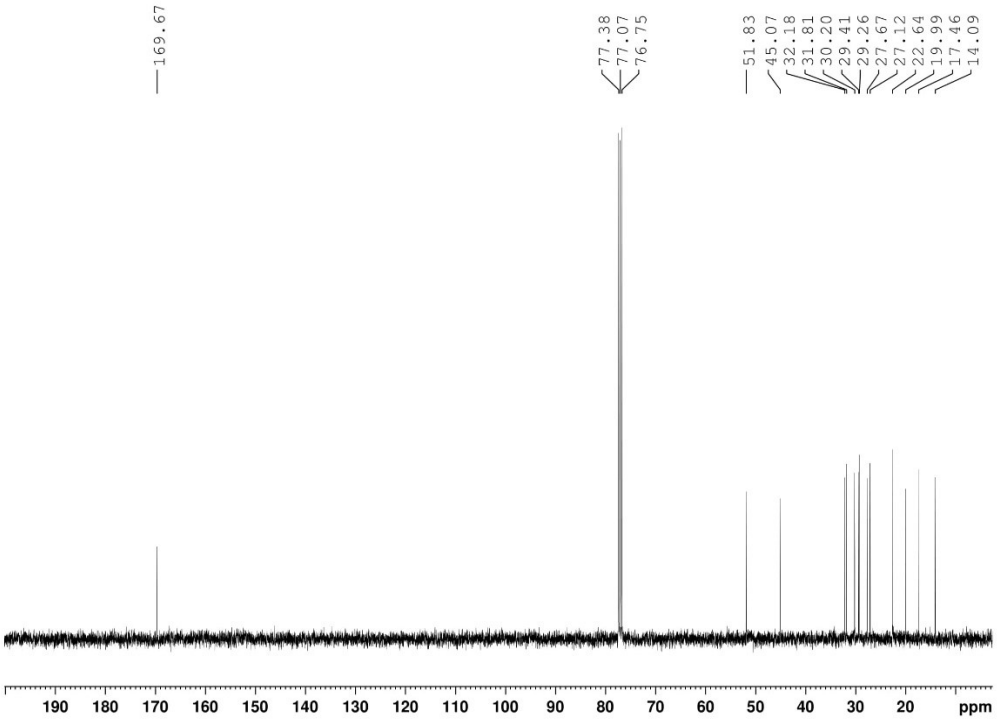

References:

1 O. Metin, X. Sun and S. Sun, *Nanoscale*, 2013, **5**, 910–912.
2 Z. Xi, J. Li, D. Su, M. Muzzio, C. Yu, Q. Li and S. Sun, *J. Am. Chem. Soc.*, 2017, **139**, 15191-15196.
3 S. Peng, Y. Lee, C. Wang, H. Yin, S. Dai and S. Sun, *Nano Res.*, 2008, **1**, 229–234.
4 J. D. Vidal, M. J. Climent, P. Concepcion, A. Corma, S. Iborra and M. J. Sabater, *ACS Catal.*, 2015, **5**, 5812–5821.
5 J. D. Vidal, M. J. Climent, A. Corma, D. P. Concepcion and S. Iborra, *ChemSusChem*, 2017, **10**, 119–128.
6 T. Zhang, Y. Ge, X. Wang, J. Chen, X. Huang and Y. Liao, *ACS Omega*, 2017, **2**, 3228–3240.
7 J. Zhang, B. Xie, L. Wang, X. Yi, C. Wang, G. Wang, Z. Dai, A. Zheng and F. S. Xiao, *ChemCatChem*, 2017, **9**, 2661–2667.
8 X. L. Du, L. He, S. Zhao, Y. M. Liu, Y. Cao, H. Y. He and K. N. Fan, *Angew. Chemie - Int. Ed.*, 2011, **50**, 7815–7819.
9 A. S. Touchy, S. M. A. Hakim Siddiki, K. Kon and K. I. Shimizu, *ACS Catal.*, 2014, **4**, 3045–3050.
10 S. M. A. H. Siddiki, A. S. Touchy, A. Bhosale, T. Toyao, Y. Mahara, J. Ohyama, A. Satsuma and K. I. Shimizu, *ChemCatChem*, 2018, **10**, 789–795.
11 G. Chieffi, M. Braun and D. Esposito, *ChemSusChem*, 2015, **8**, 3590–3594.
12 Y. B. Huang, J. J. Dai, X. J. Deng, Y. C. Qu, Q. X. Guo and Y. Fu, *ChemSusChem*, 2011, **4**, 1578–1581.
13 Y. Wei, C. Wang, X. Jiang, D. Xue, J. Li and J. Xiao, *Chem. Commun.*, 2013, **49**, 5408-5410.
14 Y. Wei, C. Wang, X. Jiang, D. Xue, Z. T. Liu and J. Xiao, *Green Chem.*, 2014, **16**, 1093-1096. 13